Thermochronologic perspectives on the deep-time evolution of the deep biosphere

Henrik Drake[a,1] and Peter W. Reiners[b,1]

[a]Department of Biology and Environmental Science, Linnæus University, Kalmar 391 82, Sweden; and[b]Department of Geosciences, University of Arizona, Tucson, AZ 85721

Edited by Susan L. Brantley, Pennsylvania State University, University Park, PA, and approved September 8, 2021 (received for review May 24, 2021)

The Earth's deep biosphere hosts some of its most ancient chemolithotrophic lineages. The history of habitation in this environment is thus of interest for understanding the origin and evolution of life. The oldest rocks on Earth, formed about 4 billion years ago, are in continental cratons that have experienced complex histories due to burial and exhumation. Isolated fracture-hosted fluids in these cratons may have residence times older than a billion years, but understanding the history of their microbial communities requires assessing the evolution of habitable conditions. Here, we present a thermochronological perspective on the habitability of Precambrian cratons through time. We show that rocks now in the upper few kilometers of cratons have been uninhabitable (>~122 °C) for most of their lifetime or have experienced high-temperature episodes, such that the longest record of habitability does not stretch much beyond a billion years. In several cratons, habitable conditions date back only 50 to 300 million years, in agreement with dated biosignatures. The thermochronologic approach outlined here provides context for prospecting and interpreting the little-explored geologic record of the deep biosphere of Earth's cratons, when and where microbial communities may have thrived, and candidate areas for the oldest records of chemolithotrophic microbes.

deep biosphere | deep time | evolution | thermochronology | extremophiles

Research in the last few decades has revealed a vast global rock- and sediment-hosted subsurface biosphere in marine sediments, hydrothermal vents at midocean ridges, porespace and fractures in oceanic crust and continental sedimentary rocks, and fracture systems of continental igneous and metamorphic rock (1–3). Most current estimates show that this deep biosphere hosts the majority of microbial life on Earth (estimated ~90% of bacteria and archaea) and about 10 to 20% of all terrestrial biomass (4–6). These communities compose a large but variable part of unclassified microbial "dark-matter" metagenome and subsurface phyla with no known closely related surface relatives, and they thrive independently of the surface photosphere (7–10). Metabolic activity at great depth in this vast, dark, and largely anoxic environment relies largely on abiotic, energy-yielding chemolithotrophic reactions, including oxidation of abiotic H_2 (1), methanogenesis, and sulfate reduction (7), and on recycling of metabolic waste products (11). Shallower parts of these ecosystems are dominated by heterotrophic communities that utilize descending dissolved organic carbon (12).

The abundance of cells in the subsurface decreases with depth in both marine (13) and continental environments (5) due to decreasing surface-derived carbon and increasing temperatures. Higher metabolic rates and biomass generation are observed (e.g., for methanogens and methanotrophs) at temperatures below ~85 °C (14, 15). At depths where temperatures approach and exceed 100 °C, hyperthermophiles dominate (14), but these also require temperatures below about 121 to 122 °C (16, 17).

Evidence from fluid inclusions and molecular dating suggest that microbial methanogenesis originated early on Earth (18, 19), and methanogens have been proposed as one of the primary life forms, evolving before phototrophs like cyanobacteria (20). Life at earth's surface proliferated in the Ordovician, and it has been proposed that before the plant colonization of the continents, life in the subsurface composed the majority of biomass (21). Yet, there is very little knowledge of when life colonized the deep subsurface of the fractured crust and for how long the communities and metabolisms of the deep rock–hosted biosphere may have evolved and persisted (22).

Of particular interest for these questions and their astrobiological implications (22) are some of the oldest terrestrial rocks, which are exposed on all continents in Precambrian cratons. Recent applications of microscale stable isotope techniques, surveys for preserved organic molecules, and geochronology of mineral precipitates in fluid-filled fractures have revealed evidence for ancient microbial methanogenesis, methane oxidation, and sulfate reduction in one craton, the Fennoscandian Shield (23, 24). This shows the potential for reconstructing the history of deep-time subsurface microbial activity, but we currently lack a useful conceptual framework and geologic context for predicting and prospecting for potentially long-lived and evolutionarily informative deep chemolithotrophic life in these environments.

Recent work using radiogenic noble-gas isotopes suggests that brines in isolated pockets of the deep fracture networks within Archaean basement rocks may have residence times of 10^7 to 10^9 y (25). Examples include 2.8-km-deep fluids isolated from the photosphere since ~25 million years (Ma) (26)

Significance

The Earth's deep biosphere is one of the least explored and understood environments. It hosts microbial lineages that are of interest for understanding the origin and evolution of life on our planet. Understanding the history of these microbial communities requires assessing the complex evolution of habitable conditions. This study presents the first thermochronological perspective on the habitability of Earth's Precambrian cratons through time and suggests that the longest record of continuous habitability to the present does not stretch much beyond 1 billion years. This thermochronologic approach provides context for prospecting and interpreting the little-explored geologic record of the deep biosphere of Earth's cratons and points to candidate areas for the oldest records of subsurface microorganisms.

Author contributions: H.D. and P.W.R. designed research, performed research, analyzed data, and wrote the paper.

The authors declare no competing interest.

This article is a PNAS Direct Submission.

[1]To whom correspondence may be addressed. Email: henrik.drake@lnu.se or reiners@arizona.edu.

This article contains supporting information online at http://www.pnas.org/lookup/suppl/doi:10.1073/pnas.2109609118/-/DCSupplemental.

Published November 1, 2021.

in a South African gold mine carrying extant chemolithotrophic microbes (27), and 2.5-km-deep saline fluids with 20- to 50-Ma residence times from the Outokumpu deep drill hole in Finland contain active archaeal and bacterial communities (28). In the Canadian Shield, fracture fluids from 2.4- and 2.9-km depths in Ontario's Kidd Creek Mine have mean residence times of as old as 1.1 to 1.7 billion years (Ga) (25) and 1.0 to 2.2 Ga (29), respectively. Younger residence times (200 to 900 Ma) are interpreted for fracture fluids from mines in Sudbury, Ontario, hosted by rocks formed by meteorite impact at 1.85 Ga (29).

However, fluid residence times provide only limited constraints on potential microbial habitation histories, and extant biologic activity in a given setting is not necessarily directly descended from ancient ancestors of the same local environment. Cell counts and culture-based methods indicate active archaeal and bacterial communities in the fracture fluids in Kidd Creek mine (30), and clumped isotope signatures suggest microbial methanotrophy at 2.4-km depth (31). Signatures of mass-independent sulfur isotope fractionation in the deep Kidd Creek fluids suggest a long-standing sulfur cycle but likely reflect oxidation of wall rock sulfides postdating the Archaean ore formation (32). While multiple lines of evidence provide intriguing suggestions that microbial life in this and other settings may be old, there are currently few constraints on the timing of active microbial habitation. For the Kidd Creek location, Li et al. (32) state that the crustal section has been at the same depth over the past 2 Ga, based on estimates of limited denudation of the shield rocks since this time (33). However, as we show here, the thermochronologic record suggests that this and other cratons (34, 35) likely experienced complex burial and exhumation histories, with important implications for their habitation history.

Here, we present a previously unexplored thermochronological deep-time perspective to interpreting the temperature-controlled habitability of the Precambrian cratons on earth. This framework builds on the recent advances in intermediate- and low-temperature thermochronology and is coupled to radioisotopic dating constraints on mineral-hosted biosignatures in cratons, where they have been documented thus far. This approach predicts the temporal and regional distribution and history of ancient and currently habitable conditions, as well as high-temperature burial episodes, in the upper continental crust, and points to craton locations most likely to feature the longest record of isolated microbial chemolithotrophic evolution on Earth.

Results and Discussion

Thermochronologic Approach. Our work takes advantage of recent interpretational advances in intermediate- and low-temperature thermochronology that have improved resolution of thermal histories (time-temperature, or *t-T* paths) of the uppermost few kilometers of crustal sections over 10^7- to 10^9-y timescales (34, 36). For all cases shown here, key constraints come from $^{40}Ar/^{39}Ar$ dating, constraining *t-T* paths from ∼400 to 300 °C through ∼250 to 150 °C, as well as fission-track and (U-Th)/He techniques, using track-length distributions and variations in radiation-damage effects among crystals within single rock samples (37–39), providing *t-T* constraints through ∼30 to 120 °C, or ∼1 to 4 km, precisely the range of most interest to the history of ancient microbial habitability. The vertical length scale of temperature-controlled habitable conditions of the upper crust is roughly defined by the geothermal gradient, which in stable cratons is around 20 to 30 °C km^{-1} (40), which means the upper 3.7 to 5.6 km may be cooler than 112 °C, which is in line with microbial observations from cratons (41). When the craton is buried by sediments, the ecosystem will adapt by vertical migration of microbial consortia upwards, relative to the rock, though it may remain stationary with respect to depth beneath the surface. Similarly, during exhumation, microbial communities will appear to migrate downward through the crust, even if their depth distribution remains fixed relative to the surface. In our following assessment of the histories of habitability of cratons, we first consider the thermochronologic record of the Canadian Shield, as this is the location of the oldest deep continental fluids yet described and also an area where a relatively rich thermochronology dataset exists. Second, we describe the case of the Fennoscandian Shield where the thermochronology record can be tied to coupled biosignature-environmental-geochronology information in veins, to detect multiple periods of habitable conditions, and third, we use the same approach for other cratons where basically only thermochronology data exist.

Potential Habitability of the Canadian Shield. The Canadian Shield hosts the oldest deep continental fluids yet described. Igneous and metamorphic rocks of this and similar shields formed at high temperatures, from magmatism or deep tectonic burial commonly associated with continental or continent-arc collisions, typically followed by cooling due to exhumation of the now-exposed rock to the shallow crust (34). This evolution is characteristic of most of the south-central Canadian Shield samples shown in Fig. 1. Some regions, including southern Baffin Island, East Athabasca, and part of the Superior craton (42), cooled to near-surface temperatures (<∼50 °C) between ∼2 Ga to 1.2 Ga, followed by heating to >100 to 200 °C by ∼1.2 to 0.9 Ga (Fig. 1*B*). This reheating is most likely due to burial by sedimentary rocks. This history is shared by samples from most Canadian Shield locations including more central and eastern portions, though in some cases it is only possible to confidently constrain the *t-T* path subsequent to the last cooling episode because identifying nonmonotonic cooling histories requires data from certain types of thermochronometric approaches not yet available in all cases. Where resolved, reheating episodes are generally followed by slow cooling that brought now-exposed rocks to temperatures associated with the uppermost 2 to 3 km. The timing of ultimate cooling of the upper crust to habitable conditions (<∼100 to 120 °C) after burial phase varies regionally. Thermochronologic constraints from samples near the Kidd Creek mine (Fig. 1*A*) and its isotopic biosignatures associated with ancient crustal fluids are shown in Fig. 1*B*. Histories for most locales in the Superior and nearby cratons rule out microbial habitation earlier than ∼500 Ma for most cases. However, the western Superior ("70") and Musselwhite locales allow the possibility of cooling below 100 °C as early as 700 to 1,000 Ma. In any case, for any of these regions surrounding Kidd Creek, the thermochronologic constraints point to final cooling to habitable conditions much more recently than the mean residence times reported for the fluids in the mine (25, 29). Taken together, the existing thermochronology *t-T* models for the Canadian Shield suggest regionally variable, and in some case multiple, episodes of habitability punctuated by reheating to inhabitable temperatures, but these should ideally be compared with—yet lacking—geochronologically dated ancient biosignatures in deep fracture settings.

Coupling Deep-Time Habitability to Dated Biosignatures—The Fennoscandian Shield. While thermochronologic constraints aid interpretations of habitability through time, geochronological advances provide more direct constraints on the age of formation of minerals containing isotopic biosignatures in deep fracture networks. These include high spatial-resolution approaches such as carbonate U-Pb and Rb-Sr dating by laser-ablation inductively coupled plasma–mass spectrometry (23, 24, 43, 44). So far, dated ancient biosignatures in craton fracture networks are limited to the Fennoscandian Shield. Here, we couple this biosignature

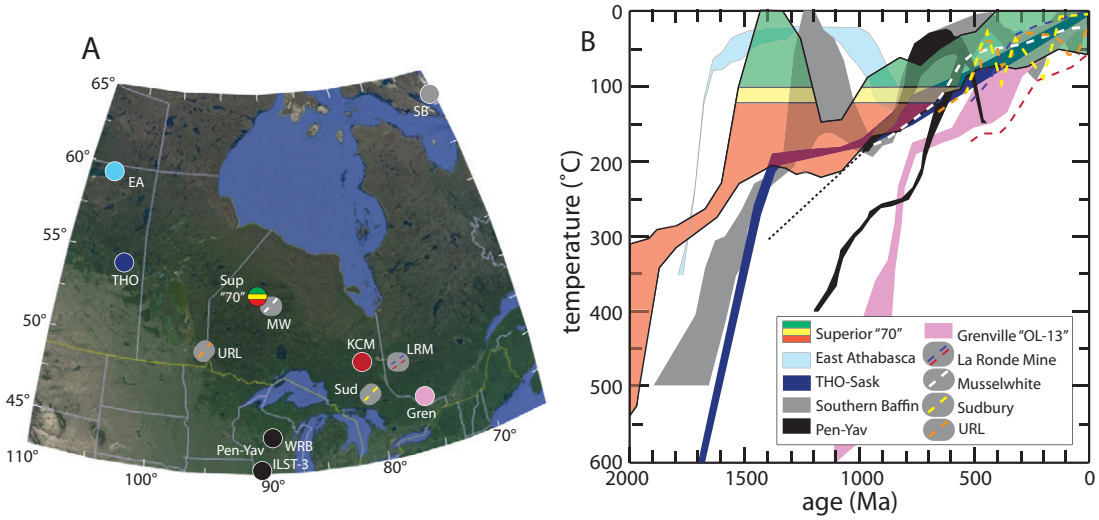

Fig. 1. Locations and model thermal histories of surface or near-surface crystalline basement rocks in the southern Canadian Shield and surrounding regions. (*A*) Location of Kidd Creek Mine (KCM, red-filled circle) and samples with thermal histories represented in *B*. (*B*) Model thermal histories. Histories constrained by multiple thermochronometers are shown as solid colors, whereas those constrained by only AFT data are shown as dashed lines. Sample Superior (Sup) "70" is from the same craton as Kidd Creek and has the longest-term, best-constrained history based on constraints from multiple thermochronometers and permitting reheating (from ref. 42) and thus is shown with green portions of histories with temperatures <100 °C, yellow for 100 to 120 °C, and red for >120 °C, delineating optimal, marginal, and uninhabitable temperature ranges for microbial activity, respectively. Other histories are as follows: East Athabasca (EA), constrained by K-feldspar $^{40}Ar/^{39}Ar$ and zircon and apatite (U-Th)/He data (34, 36, 66); Trans-Hudson Orogen (THO-Sask), from stratigraphic, U-Pb, $^{40}Ar/^{39}Ar$, and (U-Th)/He dates on multiple phases for each system (42); Pen-Yav, composite histories from U/Pb and $^{40}Ar/^{39}Ar$ on multiple phases from two samples from the southern Lake Superior region, in Wolf River Batholith of the Penokean Province, Wisconsin (WRB), and northern Yavapai province, northernmost Illinois (ILST-3) (67); Grenville OL-13 (Gren), based on titanite U/Pb and hornblende and biotite $^{40}Ar/^{39}Ar$ and zircon and apatite (U-Th)/He ages from nearby samples (42); Southern Baffin (SB), based on K-feldspar $^{40}Ar/^{39}Ar$ and zircon and apatite (U-Th)/He data (68); Musselwhite (MW), from AFT of samples at 0.8- to 1.0-km depth in mine borehole (69); La Ronde Mine (LRM), from AFT on surface sample (blue) and 3-km depth (red) (70); Sudbury (Sud), from AFT on near-surface sample in Sudbury borehole (71, 72); URL, From AFT on a near-surface sample in the Underground Research Laboratory borehole (73).

record, including information from older hydrothermal veins, with the thermochronologic record to understand the shield's habitation history (Fig. 2).

As in the Canadian Shield, different parts of the Fennoscandian Shield show slightly different *t-T* evolution depending on regional geologic histories. We focus primarily on southern Sweden where most dated biosignatures exist, but we also show *t-T* histories for Finland and the older rocks of the Kola Peninsula. We also note that fission-track-modeling–based thermal histories of the northern Scandes, including northwest coastal and interior Lapland regions, are similar to those shown, except for regions on the far northwest coast that were reheated to ∼100 to 120 °C between about 60 to 50 Ma (45).

For southern Sweden, *t-T* constraints for the Laxemar-Äspö area are shown as green/yellow/red fields (colors representing microbial habitability with respect to temperature) encompassing best-fit histories from inverse modeling of (U-Th)/He data with geologic constraints (35). The modern surface here exposes 1.8-Ga igneous granitoids (46) intruded at ∼1,430 Ma by laccolithic granites at depths of ∼4 to 8 km (47). Erosional denudation of the igneous crust and removal of Mesoproterozoic Jotnian sediments deposited over large areas of the shield (48) continued until ∼1.1 to 1.0 Ga, when thermochronologic data permit near-surface residence of the presently exposed rock (Fig. 2*B*). At about this time, the Sveconorwegian orogeny affected the western part of the shield, depositing thick foreland sediments in the eastern part and burying previously near-surface rocks to inhabitable temperatures by 900 Ma (Fig. 2*B*). Erosional exhumation then formed a low-relief surface that was subsequently buried by Cambro-Silurian platform sediments before the main Caledonian orogeny "Scandian" collision and subsequent orogenic collapse around 430 to 380 Ma (49). Collision was again accompanied by foreland-sediment burial of the craton to depths where temperatures of presently exposed crust exceeded habitable conditions by ∼350 Ma (35, 50). Subsequent exhumation and cooling are constrained by both (U-Th)/He and Apatite Fission Track (AFT) thermochronology (Fig. 2*B*), with cooling below ∼100 °C around 250 Ma. Conditions remained within the habitable zone thereafter, with possibly a few discrete burial periods affecting some parts of the shield until basement exposure, possibly as late as in the Pliocene (51, 52).

Ages and compositions of minerals crystallized in fracture networks at different stages of this history provide complementary constraints that largely support the thermochronologic interpretations and biosignature evidence for evolution of deep habitability in the Fennoscandian Shield. The conceptual understanding of key episodes of the upper crust of south Sweden (Laxemar-Äspö area), based on fluid inclusion microthermometry, radioisotopic dating, microtextures, and stable isotopic biosignatures, is shown in Fig. 3. In this area, the first pervasive brittle vein mineral precipitation occurred during intrusion of the Mesoproterozoic granite intrusions. Minerals in hydrothermal veins from this stage have fluid inclusion homogenization temperatures of 200 to 430 °C (53) and no biogenic stable isotope compositions (Fig. 3*A*), consistent with the thermochronological predictions of temperatures too high for microbial colonization at the time (Fig. 2*B*). During the subsequent Sveconorwegian orogenic event, the rock volume was exhumed to shallower crustal levels (Fig. 3*B*). Although the thermochronologic constraints permit possible habitability at this time (Fig. 2*B*), no isotopic biosignatures have yet been reported for minerals in strike-slip faults activated in the craton east of the orogeny (54). After a cycle of foreland-basin–related burial and subsequent erosion and exhumation, the early Paleozoic Caledonian orogenic event is recorded by ∼400-Ma Rb-Sr

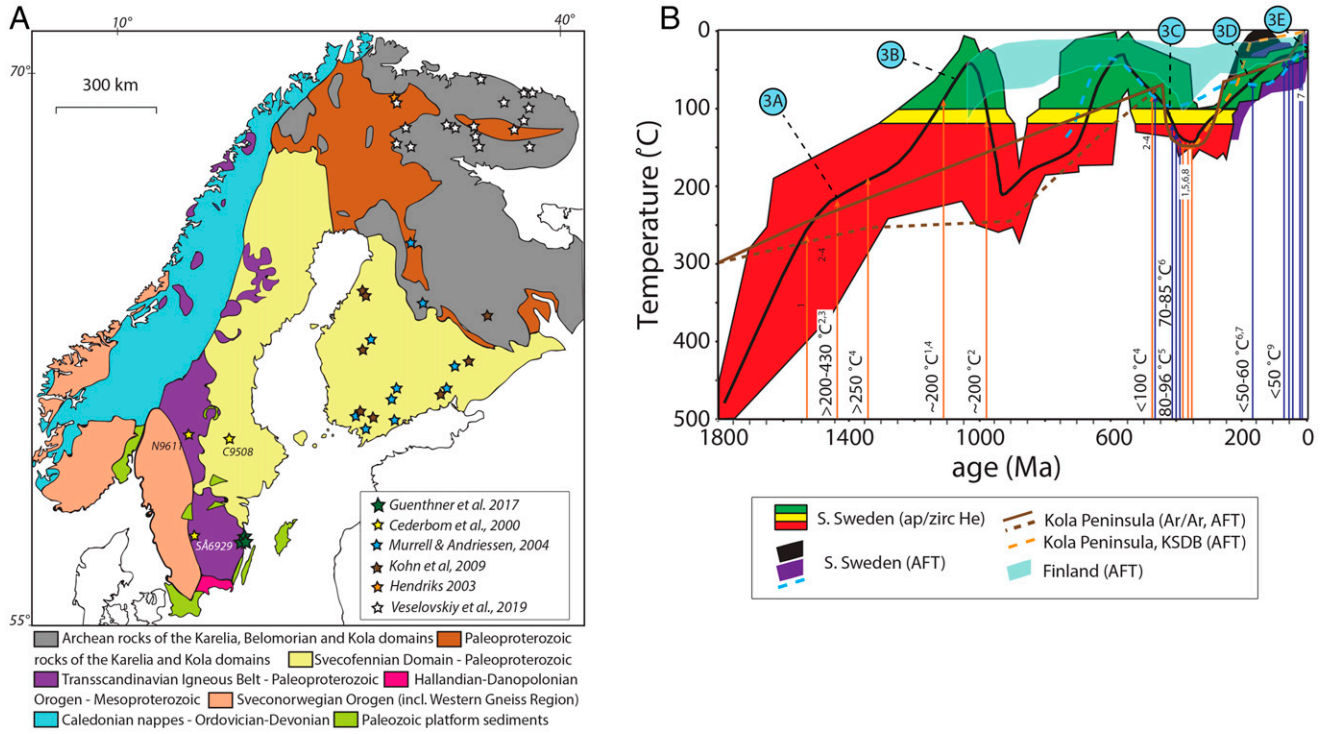

Fig. 2. Representative thermal histories of present-day surficial crystalline basement rocks in the Fennoscandian Shield. Southern Sweden: (*A*) Geological map with sample locations. (*B*) Thermal histories, including the following: 1) Constraints from Laxemar-Äspö area are shown as field encompassing best-fit inverse histories from inverse modeling of zircon and apatite (U-Th)/He dates and date-eU correlations (35). Green portions represent temperatures <100 °C, yellow for 100 to 120 °C, and red for >120 °C, delineating optimal, marginal, and inhabitable temperature ranges for microbial activity, respectively. Bold black trend through this field is mean of best-fit thermal histories. 2) Black and purple fields at <300 Ma are possible *t-T* histories from AFT data involving both monotonic and reheating histories from samples N9611 and SA9629, and dashed blue trend is best-fit history for sample C950847. Kola Peninsula: 1) Brown trends are fits to combined $^{40}Ar/^{39}Ar$ dating of hornblende, mica, and feldspar, with AFT. Solid trend is central Kola terrane, and dashed trend is for northeastern Murmansk terrane (59). 2) Orange dashed line is best-fit thermal model for AFT data from surface sample of the Kola Superdeep Borehole. Finland: partially transparent blue field is amalgamation of best-fit *t-T* histories from AFT, modified to allow for higher temperature reheating (up to ~110 °C) between ~400 to 600 Ma as represented in AFT track length modeling of samples from southern Finland (60). Symbols 3A–E in *B* are *t-T* positions in focus in Fig. 3. Other supporting references are provided in *SI Appendix*.

ages in reactivated fractures containing minerals with brine-type fluid inclusion homogenization temperatures of 70 to 96 °C and the earliest record of isotopic biosignatures (Fig. 3*C*) (24, 55). Burial-related heating is interpreted to have been accompanied by expulsion of bitumen and seep oils from black shales in the overlying sedimentary pile into the deeper basement fracture network where they provided energy for microbial communities (Fig. 3*C*) (24). By ~350 Ma, deeper burial by foreland basin sediments had heated the crystalline basement to temperatures higher than microbial habitability (Fig. 2*B*), consistent with vein fluid inclusions homogenization temperatures up to 140 °C (56). It is notable, however, that these ~400 Ma biosignatures fall on a best-fit (U-Th)/He thermochronology model that is too hot for, or possibly just on the border of, habitability. This suggests that ranges of possible *t-T* paths, rather than best-fit curves, are more suitable for assessing potential habitability. It is also important to consider that the temperatures in the fracture fluids (the potential microbial habitats) may be a bit different from those of the wall rock minerals, such as during ascent of hot hydrothermal fluids from below or nearby magmatic systems. However, for the Fennoscandian Shield periods with detected biosignatures, there are no magmatic activity, and fluid inclusion homogenization temperatures of the vein minerals match well with the *t-T* models of the wall rock, as described above. Hence, we do not consider the difference in temperature between the fracture habitats compared to the wall rock to be significant. Post-Caledonian erosion continued to reduce the thickness of the sedimentary cover, allowing deeper inflow of fresh water at about the same time as extension-related deep basement fracture development in the Jurassic. During this episode (Fig. 3*D*), carbonate minerals bearing ^{13}C-depleted isotopic signatures diagnostic of anaerobic oxidation of methane formed in the deep fracture systems at temperatures <60 °C (24). Pyrite with S-isotopic compositions diagnostic of sulfate-reducing bacteria also formed in this same generation of fracture fill. The Jurassic event was followed by several Neogene fracture reactivation and precipitation events forming authigenic carbonate formed following methanogenesis, methane oxidation, and marine/meteoric water infiltration in the fracture systems of the Siljan impact crater (23), and at Laxemar-Äspö (43), which diluted and flushed out the brine groundwater. Following complete sedimentary cover removal, the bedrock fracture systems were subject to repeated Quaternary glacial meltwater inflow and further brine flushing (57) (Fig. 3*E*).

These geobiological constraints in fractures show a mineral record of transient periods of microbial activity, such as activity of methanogens, methanotrophs, and sulfate reducers, that is largely consistent with thermochronologic constraints and points to episodic habitability only when the presently exposed rocks were sufficiently shallow and cool and when descending waters with low salinity infiltrated fracture systems and mixed with older brines. Taken together, the thermochronology record suggests that southern Sweden has a history of more or less continuously habitable conditions that date back ~250 Ma but that older episodes of habitability, recorded by Devonian vein

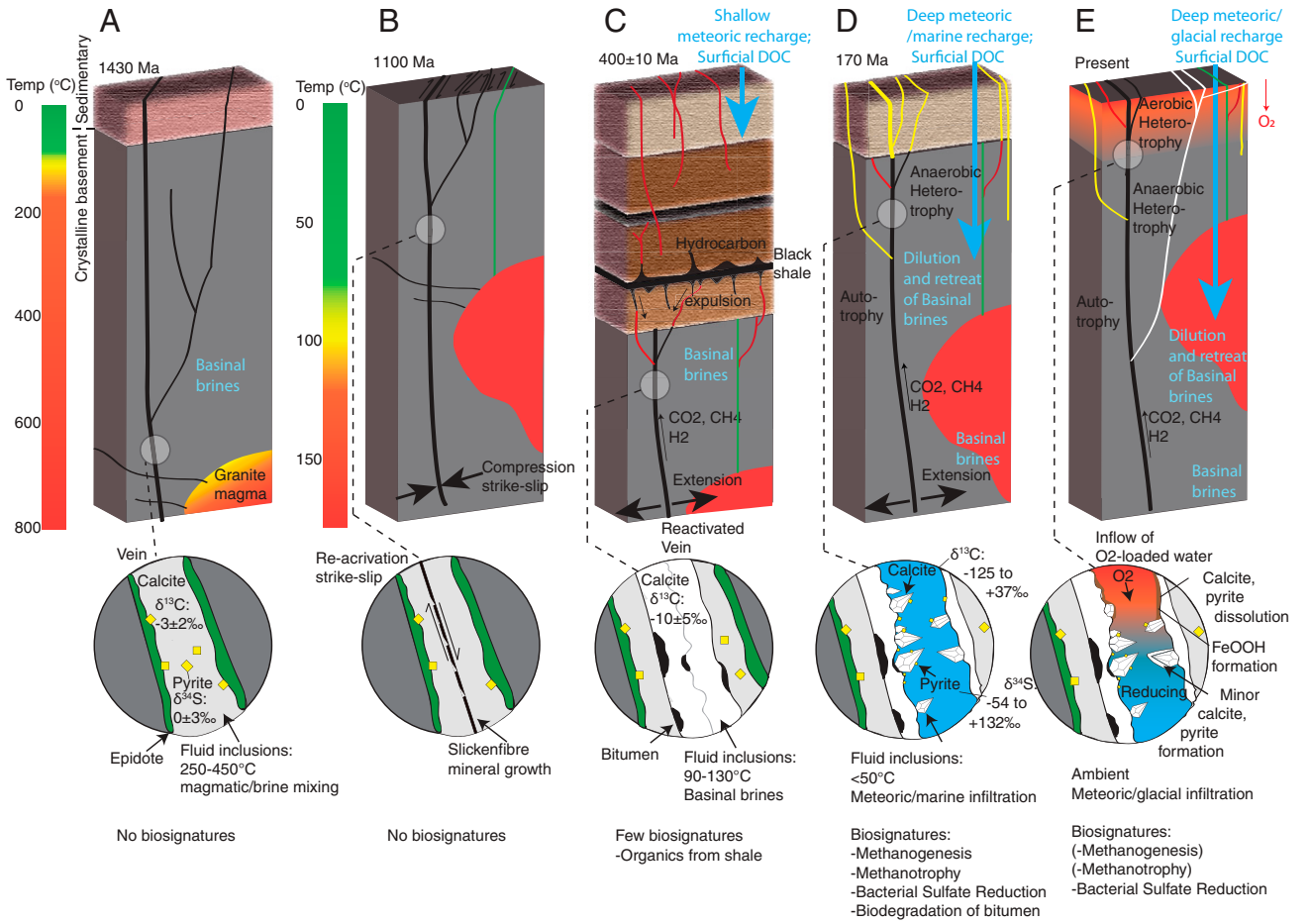

Fig. 3. Schematic evolution of the exhumation and burial history of southern Fennoscandian Shield. Key stages (*A–E*) are shown with a record of biosignatures, environmental and geochronology information, that includes fracturing events (different colors for each event), mode of fracturing (extension or strike-slip), fluid inclusions of mineral veins (homogenization temperatures and equivalent salinity), stable isotopes in vein minerals ($\delta^{13}C$ of calcite, $\delta^{34}S$ of pyrite), minerals precipitated and dissolved at different events, biosignatures detected for different microbial metabolisms (mainly by diagnostic stable C and S isotope values), and descent and ascent of heterotrophic and autotrophic substrates (e.g., DOC = dissolved organic carbon, CO_2, CH_4, and H_2) as well as water types and water mixing (24, 53–57). See text in section *Coupling Deep-Time Habitability to Dated Biosignatures—The Fennoscandian Shield* for more details. Other supporting references are provided in *SI Appendix*.

signatures, also occurred before the late Caledonian burial event. If the thermochronology models are right, we predict the presence of biosignatures in all three of the habitable windows. However, we acknowledge that the further back in time we look, the less likely biosignatures are too be found, both due to the history of the mineral veins, that is, potential mineral dissolution or insignificant mineral precipitation, or due to thermal degradation of organic molecules at the burial episodes. We also acknowledge the increased uncertainty of thermochronologic constraints, particularly those allowing nonmonotonic cooling histories, farther back in time.

The early parts of the *t-T* history of the northeastern part of Fennoscandian Shield, the Kola Peninsula, is not as well resolved as in southern Sweden, but existing data show that the Caledonian to present history affecting these Archaean to Paleoproterozoic rocks is similar, with a pre-Caledonian period of potential habitation (at ~650 to 450 Ma) followed by foreland basin burial that heated now-exposed rocks to inhabitable temperatures (58, 59) (Fig. 2*B*). The *t-T* history of the southeastern part of the shield, in southern Finland, is only constrained by apatite fission-track data, but interestingly, these provide clear evidence for temperatures lower than ~110 °C since ~1 Ga, likely due to the greater distance from the Caledonian orogenic belt (and Sveconorwegian orogenic belt) that buried more proximal parts of the foreland basin (57). Ancient biosignatures exist in the fractured igneous crust of western Finland, in the form of S- and C-isotopic compositions diagnostic of microbial activity (61, 62), but no geochronological constraints are yet available. We propose that this region may contain some of the most ancient, and possibly continuously, habitable conditions in Europe.

A Global Precambrian Shield Outlook. Although we currently lack detailed geochronological and biosignature data from Precambrian basement fracture-filling minerals in most other cratons, the approach of evaluating potential habitability in the context of "deep-time" thermochronologic constraints can be applied to other shields with thermochronological datasets in at least a preliminary way (Fig. 4). Our representation of these time periods of potential habitability in Fig. 4 focuses primarily on rocks sampled at the surface today, but in at least a few cases, we can also use distinct thermal histories of deeper samples, from drill cores or recently incised valleys, to predict the history of microbial habitation. This analysis shows that only a few places in Precambrian shields worldwide host continuously habitable subsurface conditions older than ~1 Ga. In addition to eastern

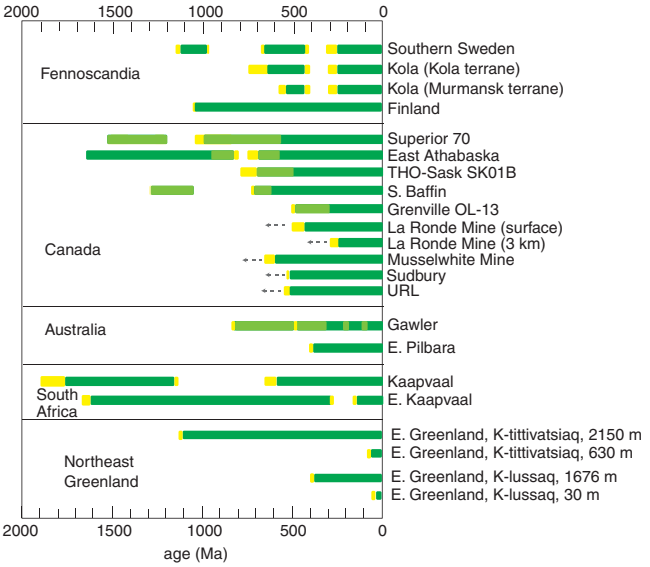

Fig. 4. Time bars of habitability for surface or near-surface rocks in a variety of cratonic regions. Timing of residence of present-day surface rocks in selected cratonal regions at temperatures below ~100 °C (green) or 120 °C (yellow). Portions of histories in which cooling paths allow for temperatures as low as <100 °C but may have been higher are shown with transparent yellow field over green. K-tittivatsiaq and K-lussaq are short for Kangertittivatsiaq and Kangerlussaq, respectively. References and further explanations are provided in *SI Appendix*.

Finland of the Fennoscandian Shield and the Superior area of the Canadian Shield, parts of East Greenland are candidates for some of the longest continuously habitable conditions. In contrast, some regions of the world's oldest cratons bear a relatively short history of habitable conditions, such as East Kaapvaal, South Africa, and, interestingly, other locations at East Greenland. Recently reported genome similarities between sulfate-reducing bacterium *Candidatus Desulforudis audaxviator* from deep borehole fluids in Africa (Kaapvaal craton) and sedimentary rocks in North America and Eurasia suggest only minimal evolution since their physical separation, likely dating back to the breakup of Pangea beginning ~165 Ma (63), which fits well with thermochronologic constraints from the East Kaapvaal craton (64, 65) (Fig. 4) showing habitable conditions since just after 200 Ma.

This analysis also makes two other potentially useful predictions. First, some regions may preserve markedly different records of paleohabitability in fracture networks over vertical distances of the scale that would allow for comparison through drill cores or regions that experienced recent deep incision. For example, rocks currently at 3-km depth in La Ronde Mine have likely been habitable to microbes since ~250 Ma, whereas surface samples may have been habitable about twice as long (Figs. 2 and 4). Similarly, in the recently incised fjords of East Greenland, high-elevation sites could record more than a billion years of continuous microbial habitation, whereas sea-level (or lower) sites may have reached habitable conditions in only the last few million years (Fig. 4). Second, thermochronological records suggest that, similar to the southern Sweden portion of the Fennoscandian Shield, currently exposed rocks in some cratons may preserve records of ancient (up to ~2 Ga) paleohabitable conditions separated by high-temperature burial episodes (Fig. 4). Understanding different biosignatures in fracture-fill minerals produced between these sterilization events could aid interpretation of metabolic evolutionary lineages through time.

Our findings show that the chemolithotrophs occupying the deep biosphere in Precambrian cratons are not necessarily as old as ages interpreted for their host fluids because even the shallowest rocks in these settings have in many cases experienced relatively recent cooling or multiple episodes of sterilization through burial–exhumation cycles that limit potentially continuous microbial habitability to the last few hundred Ma or possibly 1 Ga in a few rare cases. This means that the deep rock–hosted biosphere must have been recolonized, from surficial environments, at several times in the past. We propose that the coupled understanding of "deep time" thermochronologic constraints, coupled with radioisotopic dating of ancient veins (24) in crystalline basement, may be a useful guide for prospecting for ancient biosignatures in deep fracture networks.

Materials and Methods

This article is based on new interpretations of thermochronology and biosignature data from published works that are cited and described in the main text and *SI Appendix*. The *SI Appendix* describes detailed sample-specific information used for the general interpretations and figures in the main text.

Data Availability. All data are included in the article and/or *SI Appendix*.

ACKNOWLEDGMENTS. We acknowledge the following grants: Swedish research council (Contract 2017-05186 to H.D.) and Formas (Contracts 2017-00766 and 2020-01577 to H.D. and P.W.R.). We acknowledge constructive reviews from Kalin McDannell and two anonymous reviewers.

1. T. O. Stevens, J. P. McKinley, Lithoautotrophic microbia, ecosystems in deep basalt aquifers. *Science* **270**, 450–454 (1995).
2. K. Pedersen, Microbial life in granitic rock. *FEMS Microbiol. Rev.* **20**, 399–414 (1997).
3. T. C. Onstott *et al.*, Observations pertaining to the origin and ecology of microorganisms recovered from the deep subsurface of Taylorsville Basin, Virginia. *Geomicrobiol. J.* **14**, 353–383 (1999).
4. S. McMahon, J. Parnell, Weighing the deep continental biosphere. *FEMS Microbiol. Ecol.* **87**, 113–120 (2014).
5. C. Magnabosco *et al.*, The biomass and biodiversity of the continental subsurface. *Nat. Geosci.* **11**, 707–717 (2018).
6. Y. M. Bar-On, R. Phillips, R. Milo, The biomass distribution on Earth. *Proc. Natl. Acad. Sci. U.S.A.* **115**, 6506–6511 (2018).
7. D. Chivian *et al.*, Environmental genomics reveals a single-species ecosystem deep within Earth. *Science* **322**, 275–278 (2008).
8. M. C. Y. Lau *et al.*, An oligotrophic deep-subsurface community dependent on syntrophy is dominated by sulfur-driven autotrophic denitrifiers. *Proc. Natl. Acad. Sci. U.S.A.* **113**, E7927–E7936 (2016).
9. L. Momper, S. P. Jungbluth, M. D. Lee, J. P. Amend, Energy and carbon metabolisms in a deep terrestrial subsurface fluid microbial community. *ISME J.* **11**, 2319–2333 (2017).
10. M. R. Osburn, D. E. LaRowe, L. M. Momper, J. P. Amend, Chemolithotrophy in the continental deep subsurface: Sanford Underground Research Facility (SURF), USA. *Front. Microbiol.* **5**, 610 (2014).
11. T. L. Kieft *et al.*, Dissolved organic matter compositions in 0.6–3.4 km deep fracture waters, Kaapvaal Craton, South Africa. *Org. Geochem.* **118**, 116–131 (2018).
12. X. Wu *et al.*, Microbial metagenomes from three aquifers in the Fennoscandian shield terrestrial deep biosphere reveal metabolic partitioning among populations. *ISME J.* **10**, 1192–1203 (2016).
13. J. Kallmeyer, R. Pockalny, R. R. Adhikari, D. C. Smith, S. D'Hondt, Global distribution of microbial abundance and biomass in subseafloor sediment. *Proc. Natl. Acad. Sci. U.S.A.* **109**, 16213–16216 (2012).
14. A. L. Reysenbach, M. Voytek, R. Mancinell, *Thermophiles Biodiversity, Ecology, and Evolution* (Springer, Boston, MA, 2012).
15. V. B. Heuer *et al.*, Temperature limits to deep subseafloor life in the Nankai Trough subduction zone. *Science* **370**, 1230–1234 (2020).
16. K. Takai *et al.*, Cell proliferation at 122°C and isotopically heavy CH_4 production by a hyperthermophilic methanogen under high-pressure cultivation. *Proc. Natl. Acad. Sci. U.S.A.* **105**, 10949–10954 (2008).
17. K. Kashefi, D. R. Lovley, Extending the upper temperature limit for life. *Science* **301**, 934 (2003).
18. J. M. Wolfe, G. P. Fournier, Horizontal gene transfer constrains the timing of methanogen evolution. *Nat. Ecol. Evol.* **2**, 897–903 (2018).
19. Y. Ueno, K. Yamada, N. Yoshida, S. Maruyama, Y. Isozaki, Evidence from fluid inclusions for microbial methanogenesis in the early Archaean era. *Nature* **440**, 516–519 (2006).
20. W. F. Martin, F. L. Sousa, Early microbial evolution: The age of anaerobes. *Cold Spring Harb. Perspect. Biol.* **8**, a018127 (2015).

21. S. McMahon, J. Parnell, The deep history of Earth's biomass. *J. Geol. Soc. London* **175**, 716 (2018).
22. Y. Wang *et al.*, A methylotrophic origin of methanogenesis and early divergence of anaerobic multicarbon alkane metabolism. *Sci. Adv.* **7**, eabd7180 (2021).
23. H. Drake *et al.*, Timing and origin of natural gas accumulation in the Siljan impact structure, Sweden. *Nat. Commun.* **10**, 4736 (2019).
24. H. Drake *et al.*, Isotopic evidence for microbial production and consumption of methane in the upper continental crust throughout the Phanerozoic eon. *Earth Planet. Sci. Lett.* **470**, 108–118 (2017).
25. G. Holland *et al.*, Deep fracture fluids isolated in the crust since the Precambrian era. *Nature* **497**, 357–360 (2013).
26. J. Lippmann *et al.*, Dating ultra-deep mine waters with noble gases and ^{36}Cl, Witwatersrand Basin, South Africa. *Geochim. Cosmochim. Acta* **67**, 4597–4619 (2003).
27. L. H. Lin *et al.*, Long-term sustainability of a high-energy, low-diversity crustal biome. *Science* **314**, 479–482 (2006).
28. M. Nyyssönen *et al.*, Taxonomically and functionally diverse microbial communities in deep crystalline rocks of the Fennoscandian shield. *ISME J.* **8**, 126–138 (2014).
29. O. Warr *et al.*, Tracing ancient hydrogeological fracture network age and compartmentalisation using noble gases. *Geochim. Cosmochim. Acta* **222**, 340–362 (2018).
30. G. S. Lollar, O. Warr, J. Telling, M. R. Osburn, B. S. Lollar, 'Follow the water': Hydrogeochemical constraints on microbial investigations 2.4 km below surface at the kidd creek deep fluid and deep life observatory. *Geomicrobiol. J.* **36**, 859–872 (2019).
31. O. Warr *et al.*, High-resolution, long-term isotopic and isotopologue variation identifies the sources and sinks of methane in a deep subsurface carbon cycle. *Geochim. Cosmochim. Acta* **294**, 315–334 (2021).
32. L. Li *et al.*, Sulfur mass-independent fractionation in subsurface fracture waters indicates a long-standing sulfur cycle in Precambrian rocks. *Nat. Commun.* **7**, 13252 (2016).
33. T. J. Blackburn *et al.*, An exhumation history of continents over billion-year time scales. *Science* **335**, 73–76 (2012).
34. K. T. McDannell, R. M. Flowers, Vestiges of the ancient: Deep-time noble gas thermochronology. *Elements* **16**, 325–330 (2020).
35. W. R. Guenthner, P. W. Reiners, H. Drake, M. Tillberg, Zircon, titanite, and apatite (U-Th)/He ages and age-eU correlations from the Fennoscandian Shield, southern Sweden. *Tectonics* **36**, 1254–1274 (2017).
36. R. M. Flowers, S. A. Bowring, P. W. Reiners, Low long-term erosion rates and extreme continental stability documented by ancient (U-Th)/He dates. *Geology* **34**, 925–928 (2006).
37. R. M. Flowers, R. A. Ketcham, D. L. Shuster, K. A. Farley, Apatite (U–Th)/He thermochronometry using a radiation damage accumulation and annealing model. *Geochim. Cosmochim. Acta* **73**, 2347–2365 (2009).
38. D. L. Shuster, K. A. Farley, The influence of artificial radiation damage and thermal annealing on helium diffusion kinetics in apatite. *Geochim. Cosmochim. Acta* **73**, 183–196 (2009).
39. W. R. Guenthner, P. W. Reiners, R. A. Ketcham, L. Nasdala, G. Giester, Helium diffusion in natural zircon: Radiation damage, anisotropy, and the interpretation of zircon (U-Th)/He thermochronology. *Am. J. Sci.* **313**, 145 (2013).
40. N. Arndt, "Geothermal gradient" in *Encyclopedia of Astrobiology*, M. Gargaud *et al.*, Eds. (Springer Berlin Heidelberg, Berlin, Heidelberg, 2011), pp. 662–662.
41. L. Purkamo, R. Kietäväinen, M. Nuppunen-Puputti, M. Bomberg, C. Cousins, Ultra-deep microbial communities at 4.4 km within crystalline bedrock: Implications for habitability in a planetary context. *Life* **10**, 2 (2020).
42. K. T. McDannell, P. K. Zeitler, D. A. Schneider, Instability of the southern Canadian Shield during the late Proterozoic. *Earth Planet. Sci. Lett.* **490**, 100–109 (2018).
43. M. Ivarsson *et al.*, The fossil record of igneous rock. *Earth Sci. Rev.* **210**, 103342 (2020).
44. N. M. W. Roberts *et al.*, Laser ablation inductively coupled plasma mass spectrometry (LA-ICP-MS) U–Pb carbonate geochronology: Strategies, progress, and limitations. *Geochronology* **2**, 33–61 (2020).
45. B. W. H. Hendriks, P. A. M. Andriessen, Pattern and timing of the post-Caledonian denudation of northern Scandinavia constrained by apatite fission-track thermochronology. *Geol. Soc. Lond. Spec. Publ.* **196**, 117 (2002).
46. C.-H. Wahlgren *et al.*, "Geological description of rock domains and deformation zones in the Simpevarp and Laxemar subareas. Preliminary site description: Laxemar subarea - version 1.2" (SKB Report R-05-69, Swedish Nuclear Fuel and Waste Management Company, Stockholm, Sweden, 2006).
47. A. R. Cruden, "Emplacement mechanisms and structural influences of a younger granite intrusion into older wall rocks–A principal study with application to the Götemar and Uthammar granites. Site-descriptive modelling: SDM-Site Laxemar" (SKB Report R-08-138, Swedish Nuclear Fuel and Waste Management Company, Stockholm, Sweden, 2008).
48. L. Brander, U. Söderlund, Mesoproterozoic (1.47–1.44 Ga) orogenic magmatism in Fennoscandia; Baddelyite U-Pb dating of a suite of massif-type anothosite in S. Sweden. *Int. J. Earth Sci.* **98**, 499–516 (2008).
49. F. Corfu, T. B. Andersen, D. Gasser, The Scandinavian Caledonides: Main features, conceptual advances and critical questions. *Geol. Soc. Lond. Spec. Publ.* **390**, 9–43 (2014).
50. C. Cederbom, S. Å. Larson, E.-L. Tullborg, J. P. Stiberg, Fission track thermochronology applied to Phanerozoic thermotectonic events in central and southern Sweden. *Tectonophysics* **316**, 153–167 (2000).
51. P. Söderlund, L. J. Juez, L. M. Page, T. J. Dunai, Extending the time range of apatite (U-Th)/He thermochronometry in slowly cooled terranes; Palaeozoic to Cenozoic exhumation history of southeast Sweden. *Earth Planet. Sci. Lett.* **239**, 266–275 (2005).
52. P. Japsen, P. F. Green, J. M. Bonow, M. Erlström, Episodic burial and exhumation of the southern Baltic Shield: Epeirogenic uplifts during and after break-up of Pangaea. *Gondwana Res.* **35**, 357–377 (2016).
53. M. Tillberg *et al.*, Fractionation of rare earth elements in greisen and hydrothermal veins related to A-type magmatism. *Geofluids* **2019**, 20 (2019).
54. M. Tillberg *et al.*, In situ Rb-Sr dating of slickenfibres in deep crystalline basement faults. *Sci. Rep.* **10**, 562 (2020).
55. H. Drake *et al.*, Unprecedented ^{34}S-enrichment of pyrite formed following microbial sulfate reduction in fractured crystalline rocks. *Geobiology* **16**, 556–574 (2018).
56. H. Drake, E.-L. Tullborg, Paleohydrogeological events recorded by stable isotopes, fluid inclusions and trace elements in fracture minerals in crystalline rock, Simpevarp area, SE Sweden. *Appl. Geochem.* **24**, 715–732 (2009).
57. J. B. Gómez, M. J. Gimeno, L. F. Auqué, P. Acero, Characterisation and modelling of mixing processes in groundwaters of a potential geological repository for nuclear wastes in crystalline rocks of Sweden. *Sci. Total Environ.* **468–469**, 791–803 (2014).
58. R. V. Veselovskiy *et al.*, New apatite fission-track data from the Murmansk craton, NE Fennoscandia: An echo of hidden thermotectonic events. *Minerals (Basel)* **10**, 1095 (2020).
59. R. V. Veselovskiy *et al.*, Thermochronology and exhumation history of the northeastern Fennoscandian shield since 1.9 Ga: Evidence from ^{40}Ar/^{39}Ar and apatite fission track data from the Kola Peninsula. *Tectonics* **38**, 2317–2337 (2019).
60. G. R. Murrell, P. A. M. Andriessen, Unravelling a long-term multi-event thermal record in the cratonic interior of southern Finland through apatite fission track thermochronology. *Phys. Chem. Earth Parts ABC* **29**, 695–706 (2004).
61. E. Sahlstedt, J. A. Karhu, P. Pitkänen, M. Whitehouse, Biogenic processes in crystalline bedrock fractures indicated by carbon isotope signatures of secondary calcite. *Appl. Geochem.* **67**, 30–41 (2016).
62. E. Sahlstedt, J. A. Karhu, P. Pitkänen, M. Whitehouse, Implications of sulfur isotope fractionation in fracture-filling sulfides in crystalline bedrock, Olkiluoto, Finland. *Appl. Geochem.* **32**, 52–69 (2013).
63. E. D. Becraft *et al.*, Evolutionary stasis of a deep subsurface microbial lineage. *ISME J.* **15**, 2830–2842 (2021).
64. J. S. Baughman, R. M. Flowers, Mesoproterozoic burial of the Kaapvaal craton, southern Africa during Rodinia supercontinent assembly from (U-Th)/He thermochronology. *Earth Planet. Sci. Lett.* **531**, 115930 (2020).
65. J. S. Baughman, R. M. Flowers, Deciphering a 2 Gyr-long thermal history from a multi-chronometer (U-Th)/He study of the Phalaborwa Carbonatite, Kaapvaal craton, South Africa. *Geochem. Geophys. Geosyst.* **19**, 1581–1594 (2018).
66. R. Flowers *et al.*, Mulitistage exhumation and juxtaposition of lower continental crust in the western Canadian Shield: Linking high-resolution U–Pb and ^{40}Ar/^{39}Ar thermochronome-try with pressure–temperature-deformation paths. *Tectonics* **25**, TC4003 (2006).
67. D. Holm *et al.*, Growth, overprinting, and stabilization of Proterozoic Provinces in the southern Lake Superior region. *Precambrian Res.* **339**, 105587 (2020).
68. K. T. McDannell, D. A. Schneider, P. K. Zeitler, P. B. O'Sullivan, D. R. Issler, Reconstructing deep-time histories from integrated thermochronology: An example from southern Baffin Island, Canada. *Terra Nova* **31**, 189–204 (2019).
69. N. Pinet, K. T. McDannell, *The Ups and Downs of the Canadian Shield. 3, Additional Apatite Fission-Track Analyses from the Musselwhite, Roberto, Meadowbank and Raglan Mines, Ontario, Quebec, and Nunavut* (Geological Survey of Canada, 2020).
70. N. Pinet, *The Ups and Downs of the Canadian Shield: 2-Preliminary Results of Apatite Fission-Track Analysis from a 3.6 km Vertical Profile, LaRonde Mine* (Geological Survey of Canada, Quebec, 2018).
71. M. Lorencak, B. P. Kohn, K. G. Osadetz, A. J. W. Gleadow, Combined apatite fission track and (U–Th)/He thermochronometry in a slowly cooled terrane: Results from a 3440-m-deep drill hole in the southern Canadian Shield. *Earth Planet. Sci. Lett.* **227**, 87–104 (2004).
72. B. P. Kohn *et al.*, Visualizing thermotectonic and denudation histories using apatite fission track thermochronology. *Rev. Mineral. Geochem.* **58**, 527–565 (2005).
73. S. Feinstein, B. Kohn, K. Osadetz, R. Everitt, P. O'Sullivan, Variable Phanerozoic thermal history in the Southern Canadian Shield: Evidence from an apatite fission track profile at the Underground Research Laboratory (URL), Manitoba. *Tectonophysics* **475**, 190–199 (2009).